Toward realizing high power semiconductor terahertz laser sources at room temperature

Manijeh. Razeghi [a]

Center for Quantum Devices, Department of Electrical Engineering and Computer Science, Northwestern University, Evanston, Illinois 60208

ABSTRACT

The terahertz (THz) spectral range offers promising applications in science, industry, and military. THz penetration through nonconductors (fabrics, wood, plastic) enables a more efficient way of performing security checks (for example at airports), as illegal drugs and explosives could be detected. Being a non-ionizing radiation, THz radiation is environment-friendly enabling a safer analysis environment than conventional X-ray based techniques. However, the lack of a compact room temperature THz laser source greatly hinders mass deployment of THz systems in security check points and medical centers. In the past decade, tremendous development has been made in GaAs/AlGaAs based THz Quantum Cascade Laser (QCLs), with maximum operating temperatures close to 200 K (without magnetic field). However, higher temperature operation is severely limited by a small LO-phonon energy (~ 36 meV) in this material system. With a much larger LO-phonon energy of ~ 90 meV, III-Nitrides are promising candidates for room temperature THz lasers. However, realizing high quality material for GaN-based intersubband devices presents a significant challenge. Advances with this approach will be presented. Alternatively, recent demonstration of InP based mid-infrared QCLs with extremely high peak power of 120 W at room temperature opens up the possibility of producing high power THz emission with difference frequency generation through two mid-infrared wavelengths.

Keywords: terahertz, III-nitride, quantum cascade lasers, difference frequency generation

1. INTRODUCTION

Terahertz (THz) range is an area of the electromagnetic spectra which has lots of applications but it suffers from the lack of simple working devices which can emit and detect THz radiation, such as the high performance quantum cascade lasers [1] based on InP technology [2]. The applications for the THz can be found in astronomy and space research, biology imaging, security, industrial inspection, etc. Most of them rely on THz spectroscopy, which is in frequency domain, and/or THz imaging, which is in space and time domain.

THz spectroscopy deals with the frequency response in the THz range. For example, applications in astronomy and space studies are very important. Like all human beings, we would like to know the origin of our star: the Sun and as a consequence the Earth. The birth of galaxies and new stars is supposed to be due to a gas cooling process which allows interstellar dust clouds to collapse. Typical temperatures of this dense interstellar gas are in a range from about 10 K in the cooler regions to hundreds of Kelvin in the hotter and usually denser parts. The corresponding frequencies ($kT \sim h\nu$) range from about 200 GHz to 4 THz. As a consequence, 98% of post Big-Bang photons in a typical galaxy lie in the FIR spectral region [3]. Another example is given to applications in biology. THz spectroscopic tool has also been used to study some deoxyribonucleic acid (DNA) molecules. Detection of single base mutations of molecules has been demonstrated [4]. As we know, the evolution of species, or some genetic diseases, come from genetic mutations. This field of research is relevant and needs powerful and easy to use THz sources and detectors.

T-ray imaging uses the properties of absorption and transmission of different materials in the THz range. Information is usually presented in space and/or time domains. The imaging in this wavelength range has different applications in medicine and security. The entire THz range is strongly absorbed by all the polar liquids, like water. A picture of an

---

[a] email: razeghi@eecs.northwestern.edu

object can be realized to determine the presence of water. THz wavelengths penetrate most of dry, non-metallic and non polar objects like plastics, paper cardboard and non polar organic substance. This property added to the capability of the range to determine the chemical composition of samples. It allows us to imagine a package inspection with a chemical content mapping, and the direct industrial application of this technology is food inspection. This inspection can be realized in real time with a digital signal processor to extract compositional information for the entire object. This wavelength range seems to be a completely open for medical imaging. Both in dermatology and dentistry, this technique has yielded significant results. Two techniques are conceivable: transmission imaging of thin, clinically prepared tissue samples and reflection imaging. The first technique is practicable only *in vitro,* whereas the second one is possible *in vivo*. These two techniques are both valuable and depend on the task at hand. For dermatology purposes, detection of a cancer at the lowest layer of the epidermis can be achieved. T-ray imaging is able to give the size, the shape and the depth of the diseased tissue. The complete understanding of this detection method is still currently under development, and the chemical composition, or the different water absorptions are attributed to the change of absorption in the THz range. Last but not least, metals are totally opaque to this wavelength range. As a consequence, weapons and knifes can be detected easily by this technique of imaging. This type of security system could replace the actual X-ray system in the airport. Two main advantages are easily understandable. First, as T-ray is a non ionizing beam, this technique cannot damage any material. Secondly, a chemical spectrometer can be added to the security system in order to prevent any chemical or biological hazard.

Numerous terahertz sources exist. Some of them are system-like or facility-like, such as carcinotrons, photomixers, CO_2 laser pumped down-converters, p-type germanium laser, or free electron laser. Very high power output in milliwatt or watt is possible through these sources. However, they are bulky and expensive. A semiconductor terahertz source similar to the size of a diode laser is extremely attractive if it can deliver sufficient output power at the desired frequency. Conventional electronic devices such as resonant tunneling diodes, Gunn diodes, IMPATT diodes, experience difficulties for high frequencies above 1 THz due to both transit-time and resistance-capacitance effects. For example, recent demonstration of a room temperature resonant tunneling diode gives an output power of 10 µW at 1 THz [5]. For electronic devices, in order to reach a higher frequency, an up conversion is usually needed, which induces an even lower power output. Photonic devices, on the other hand, encounter difficulties in the low frequency end, due to the fact that the photon energy becomes increasingly smaller than the thermal fluctuation at room temperature. For example, the lowest frequency demonstrated by the THz quantum cascade laser (QCL) is 1.2 THz at 15 K [6]. Although there is no theoretical limitation for the emission energy ($h\nu$) relative to the thermal fluctuation (kT), since THz QCL operates away from thermal equilibrium, improving the operation temperature of THz QCL is still the biggest challenge. To date, the highest operation temperature of a THz QCL is 186 K at a frequency of 3.9 THz [7].

2. III-NITRIDE TERAHERTZ DEVICES

Thanks to the large longitudinal optical phonon energy (90 meV), III-Nitrides is a promising candidate for room temperature (RT) operation of THz quantum cascade lasers (QCLs). Realization of a THz QCL requires precise control over material and interfaces necessary to form the intersubband levels and allow injection via tunneling between levels.

Recently, we have demonstrated the first III-Nitride AlN/GaN SLs grown by MOCVD with near-infrared intersubband (ISB) transitions [8]. By decreasing the aluminum content in the barriers, we have extended the intersubband transitions in AlGaN/GaN SLs up-to 5.3 µm for the first time – only limited by sapphire substrate absorption (Fig. 1(a)) [9]. Recently, by switching to silicon substrate, up-to THz transitions are reported [10]. All these results motivate towards further intersubband device studies in III-Nitride materials.

In order to demonstrate a QCL, aside from the control over intersubband levels, quantum tunneling between cascading structures are of a must. After experimental demonstration of precise control over intersubband levels, the injector part of the QCLs – quantum tunneling – has been of focus. With the recent commercial availability of lattice-matched freestanding (FS) GaN substrates, we have designed lower aluminum content (20%) AlGaN/GaN active layers and improved the reliability of RTDs significantly. Most recently, we employed polarization-free-engineered AlGaN/GaN active layers on non-polar M-plane free-standing substrates that have enabled reliable and reproducible room temperature negative differential resistance in resonant tunneling diodes proving for the first time (irrespective of growth technique) that reliable and reproducible quantum tunneling is possible in III-Nitrides (see Fig. 1(b)) [11]. These recent experimental demonstrations provide motivation towards the eventual realization of RT THz QCLs based on III-Nitrides.
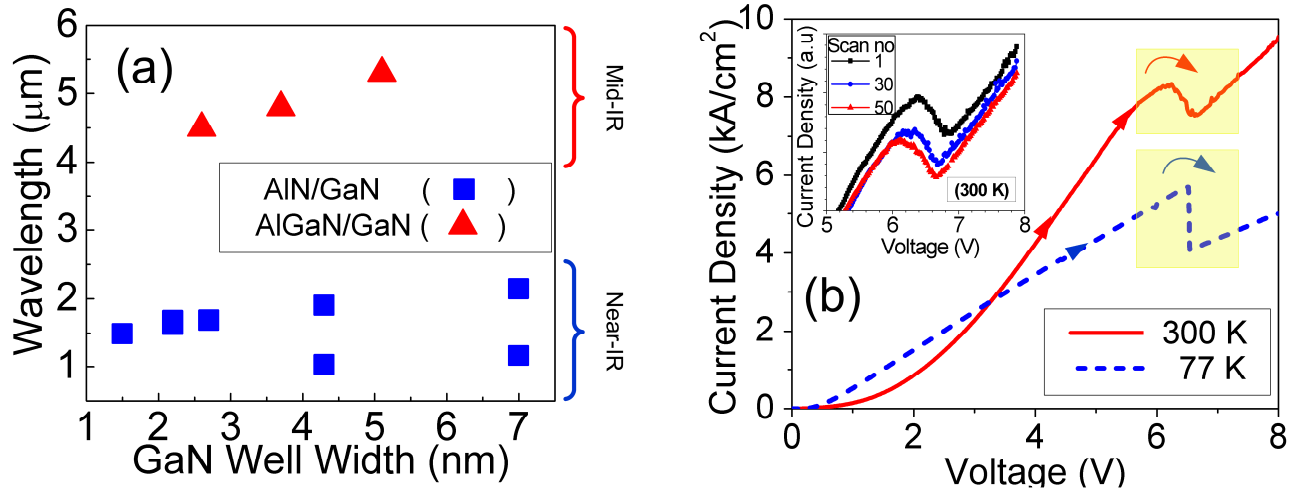
Fig. 1. (a) Demonstration of intersubband transitions in AlN/GaN and AlGaN/GaN superlattices from near-infrared to mid-infrared, respectively, and (b) room temperature (300 K) and low temperature (77 K) operation of a GaN-based resonant tunneling diode. The inset shows the reliability and reproducibility of negative differential resistance at room temperature.

3. TERAHERTZ SOURCES BASED ON INTRACAVITY DIFFERENCE FREQUENCY GENERATION

Unlike THz-QCLs, semiconductor terahertz sources based on nonlinear effects of mid-infrared QCLs do not suffer from operating temperature limitations, because mid-infrared QCLs can operate well above room temperature. DFG based terahertz sources utilize nonlinear properties of asymmetric quantum structures, such as QCL structures. Gurnick and Detemple [12] fist proposed the idea that asymmetric semiconductor quantum wells show giant nonlinear susceptibilities in 1983. Owschimikow et. al. [13] reported the first demonstration of sum frequency generation (SFG) and second harmonic generation (SHG) in QCLs. In 2007, the first terahertz QCL based on intracavity difference frequency generation (DFG) was demonstrated at 80 K [14]. Later on, room temperature operation was realized [15].

For DFG based terahertz QCLs, the biggest limitation is the power conversion efficiency. Being a second order process, the efficiency is intrinsically much lower than the first order process originating from the fundamental oscillator. Theoretical estimation is on the order of 1 mW/W^2 for the best case [14]. Experimentally, conversion efficiency around 5 μW/W^2 has been reported [15] at room temperature. The discrepancy stems from a number of practical imperfections, such as poor phase matching, high order lateral mode lasing for the mid-IR wavelengths, difficulties in collecting all the THz power, etc.

For a fixed second order power conversion efficiency, the output terahertz power increases quadratically with the increase of mid-IR power. Therefore, DFG based THz QCLs can benefit significantly from the recent dramatic power improvement of mid-IR QCLs. Shown in Fig. 2 (a) is the power performance of a broad area QCL emitting around 4.4 – 4.5 μm. The device operates at room temperature in pulsed mode with a pulse width of 200 ns and a duty cycle of 0.2%. The peak output power reaches 120 W [16]. If this mid-IR power level can be realized with a DFG device, the THz power output is expected to be enhanced by four orders of magnitude compared to a watt level mid-IR source. This means miliwatt terahertz power is well within reach with a DFG approach in QCLs, at least in room temperature pulsed mode operation.

As for room temperature continuous wave (cw) operation, the highest achieved output power is 5.1 W at a wavelength around 4.9 μm (Fig. 2(b)). Although this is significantly smaller than pulsed mode operation, it is still possible to achieve cw THz power in μW level. As continuous effort is put in improving the mid-IR power level, we are expecting a better situation for the THz emission in both pulsed and cw operations.
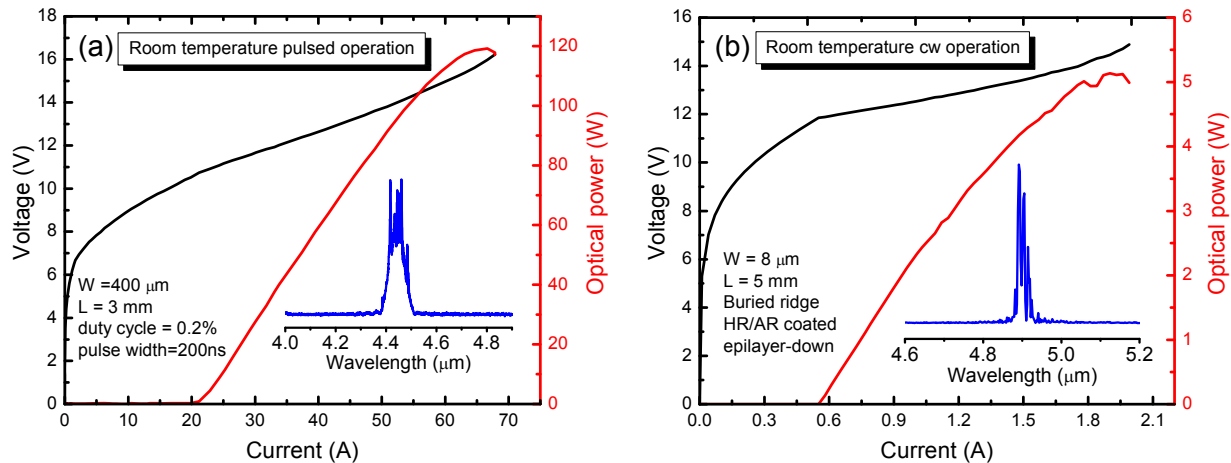
Fig. 2. (a) Room temperature pulsed mode operation of a broad area mid-IR QCL and (b) room temperature cw operation of a buried ridge mid-IR QCL. The insets are the lasing spectra measured close to the threshold.

Our first demonstration of THz DFG is based on the 9.2-10.8 μm dual-wavelength active regions [15]. The QCL structure presented in this work was grown by gas-source molecular beam epitaxy (MBE) on n-InP substrate (Si, ~ 1.5×10^{17} cm^{-3}). The growth started with 5-μm-thick InP buffer layer (Si, ~ 1.5×10^{16} cm^{-3}). The laser cores consisted of 30 stages of bound-to-continuum structures designed for the wavelength of 9.2 μm, a 100-nm InGaAs spacer (Si, ~ 1×10^{16} cm^{-3}), and 30 stages of double-phonon resonance structure designed for the wavelength of 10.8 μm. The bound-to-continuum section is also designed with a giant nonlinear susceptibility of $|\chi^{(2)}| = 4 \times 10^4$ pm/V for DFG. The growth ended with a 3.5-μm-thick InP cladding layer (Si, ~ 1.5×10^{16} cm^{-3}) a 200-nm-thick InP contact layer (Si, ~5×10^{18} cm^{-3}). Compared with [15], the lower doping levels in the InGaAs spacer, InP buffer, and cladding reduced the losses in mid-infrared (mid-IR) and THz for about 20% and 40%, respectively. The phase mismatching and coherent length are further improved by the reduced losses. The phase mismatching for this waveguide is estimated to be around 40 cm^{-1}. The THz power conversion efficiency is expected to be improved by 2.2 times given the reduced loss and phase mismatching.

The sample was processed into a double-channel geometry with a 16-μm ridge width tapered into 60 μm. 2-3 mm cavities were Y$_2$O$_3$/Au HR coated and mounted epilayer-up on copper submounts. For DFB, a dual-period grating was defined into the cap layer with a grating depth of 200 nm.

Fig. 3 (a)-(c) show the Mid-IR temperature-dependent *P-I-V* characterization, spectra at 80 K, and far field at room temperature of a tapered FP QCL with a 2-mm cavity length, a 16-μm ridge width tapered into 60 μm, and a taper angle of 1.4°. The narrow ridge width is crucial to secure fundamental transverse mode operations in the working-current and temperature ranges for the two wavelengths. This of special importance to the THz single based on DFG, since an optimal effective area of mode interaction is expected from the fundamental transverse mode operation of the two wavelengths. Any higher transverse mode operation will significantly decrease the THz signal [17]. Fig. 3 (d) shows the THz spectra at 80 K and 300 K. A Si hyperhemispherical lens is used for the room temperature tests. The THz wavelength is about 68 μm, corresponding to the mid-IR wavelength spacing of 147 cm^{-1}. Clearly, the THz signal is strongly dependent on the pumping power as the current increase or temperature decrease. The multimode behavior of the THz spectra is determined by the multimode nature of the mid-IR pumping source. This can be improved by incorporating a dual-period grating into the waveguide to purifying the spectra of the mid-IR pump.
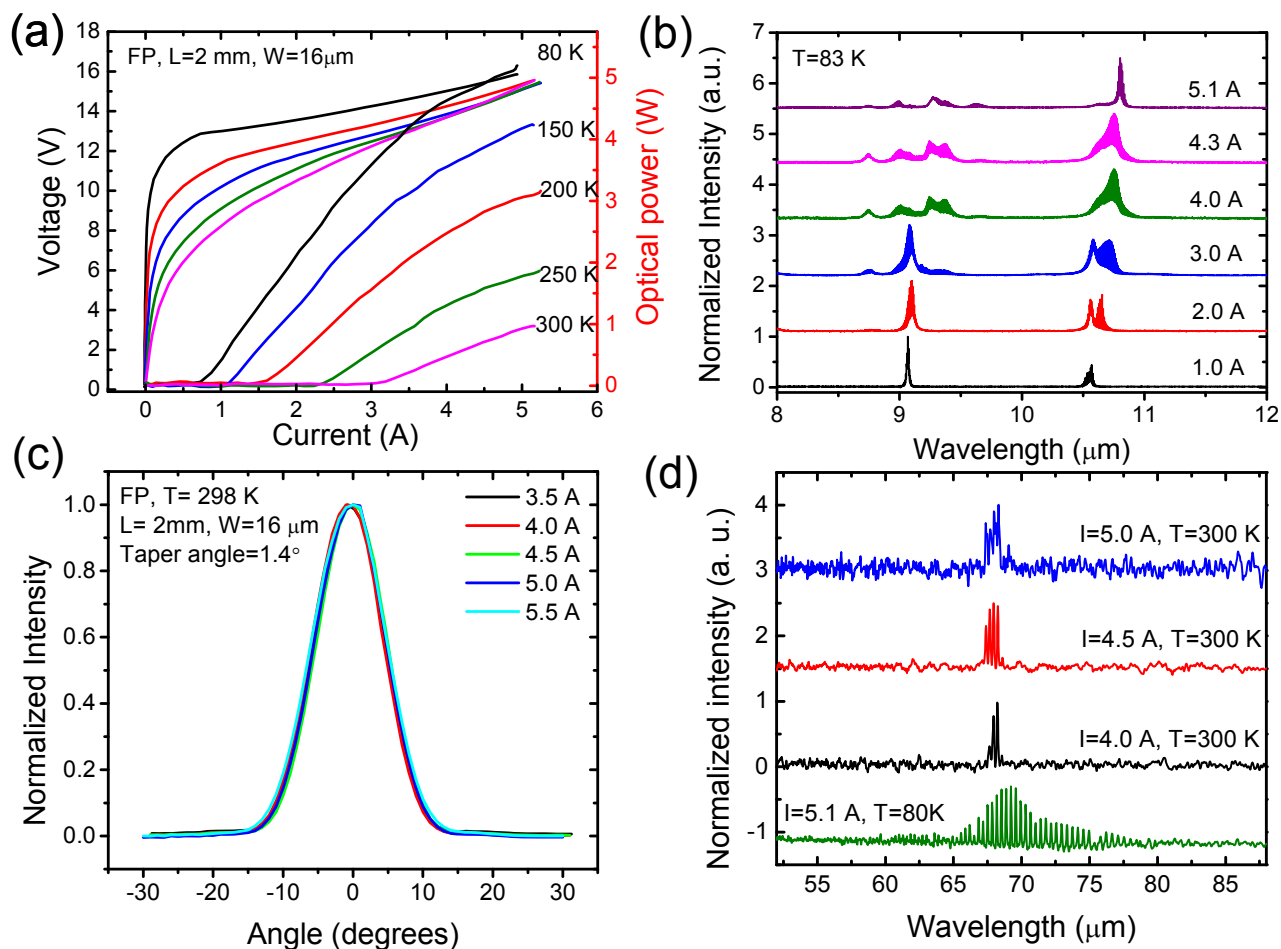
Fig. 3. (a)-(c) Mid-IR temperature-dependent P-I-V characterization, spectra at 80 K, and far field at room temperature of a tapered FP QCL with a 2-mm cavity length, 16-μm ridge width tapered into 60 μm, and a taper angle of 1.4°. (d) THz spectra at 80 K and 300 K. A Si lens is used for the room temperature tests.

Fig. 4 (a)-(b) show the Mid-IR *P-I-V* characterization and spectra at room temperature of a tapered DFB QCL with the same geometry as the FP counterpart. The power is almost reduced by 50% compared with the FP, which can be explained by the extra feedback of the grating and therefore the reduced outcoupling efficiency. The spectra is purified, however, and single mode operation for both wavelengths is obtained. Fig. 4 (c) shows the grating geometry and its Fourier transform spectrum. The two main peaks correspond to the single mode operation of the lasing spectra. Several other small peaks around the two main peaks have resulted from the truncation of the grating geometry by dry etching. Nevertheless, these peaks will not contribute to the pump spectra due the large distance from the gain peaks of the active regions. Fig. 4 (d) shows the THz spectra at different currents in 300 K. A Si lens is used for the room temperature tests. Single mode THz operation is obtained due to the single mode operation of the two pumping sources. Interestingly, the wavelength is almost fixed with different working currents. In other words, despite mild tuning of the mid-IR pump wavelengths with current/ temperature, their difference frequency remains almost constant, leading to a very stable, narrow linewidth THz source.

Transferring this technology to the short wavelengths around 4.4 – 4.5 μm, with a proper nonlinear DFG regime, are expected to give even higher performance THz emitters thanks to the high-power pumping sources.
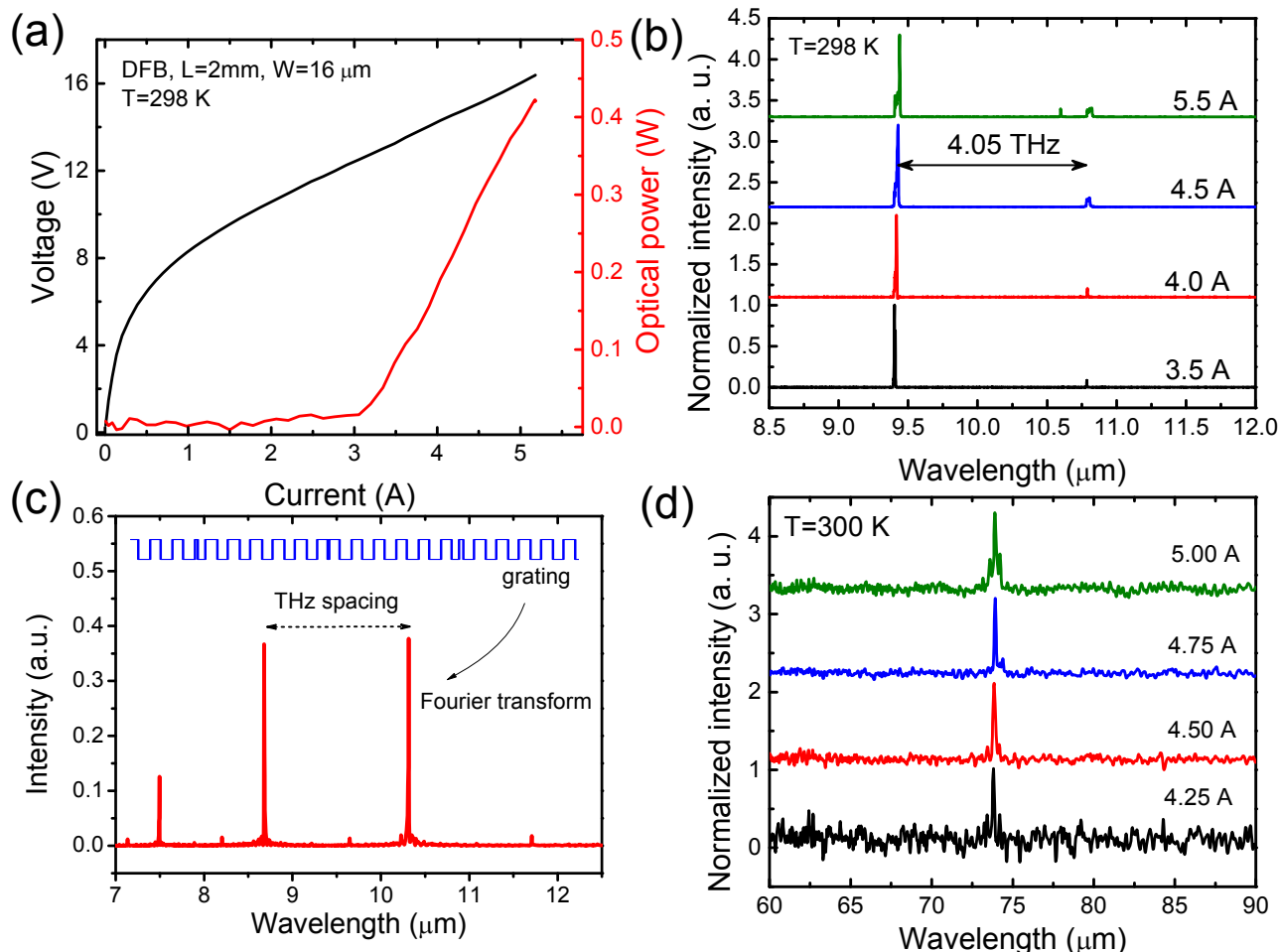
Fig. 4. (a) Mid-IR temperature dependent P-I-V characterization, (b) spectra at 80 K of a tapered DFB QCL with 2 mm cavity length, 16 μm ridge width, and taper angle of 1.4°. (c) The dual-period grating design. (d) THz spectra at 300 K.

4. ACKNOWLEDGEMENTS

REFERENCES

[1]   Razeghi, M., "High-Performance InP-Based Mid-IR Quantum Cascade Lasers," IEEE J. Sel. Top. Quantum Electron., 15, 941-951 (2009).

[2]   Razeghi, M., [The MOCVD Challenge: A survey of GaInAsP-InP and GaInAsP-GaAs for photonic and electronic device applications, Second Edition], Taylor and Francis/CRC Press, (2010).

[3]   Siegel, P. H., "Terahertz technology," IEEE Transactions on Microwave Theory and Techniques, 50, 910-928 (2002).

[4]   Nagel, M., Bolivar, P. H., Brucherseifer, M., Kurz, H., Bosserhoff, A., and Buttner, R., "Integrated THz technology for label-free genetic diagnostics," Appl. Phys. Lett., 80, 154-156 (2002).

[5]   Suzuki, S., Asada, M., Teranishi, A., Sugiyama, H., and Yokoyama, H., "Fundamental oscillation of resonant tunneling diodes above 1 THz at room temperature," Appl. Phys. Lett., 97, 242102-3 (2010).

[6]   Walther, C., Fischer, M., Scalari, G., Terazzi, R., Hoyler, N., and Faist, J., "Quantum cascade lasers operating from 1.2 to 1.6 THz," Appl. Phys. Lett., 91, 131122-3 (2007).

[7]   Kumar, S., Hu, Q., and Reno, J. L., "186 K operation of terahertz quantum-cascade lasers based on a diagonal design," Appl. Phys. Lett., 94, 131105 (2009).

[8]   Bayram, C., Pere-laperne, N., McClintock, R., Fain, B., and Razeghi, M., "Pulsed metal-organic chemical vapor deposition of high-quality AlN/GaN superlattices for near-infrared intersubband transitions," Appl. Phys. Lett. 94, 121902 (2009).

[9]   Pere-laperne, N., Bayram, C., Nguyen-The, L., McClintock, R., and Razeghi, M., "Tunability of intersubband absorption from 4.5 to 5.3 μm in a GaN/Al$_{0.2}$Ga$_{0.8}$N superlattices grown by metalorganic chemical vapor deposition," Appl. Phys. Lett. 95, 131109 (2009).

[10]   Machhadani, H., Kotsar, Y., Sakr, S., Tchernycheva, M., Colombelli, R., Mangeney, J., Bellet-Amalric, E., Sarigiannidou, E., Monroy, E., and Julien, F., "Terahertz intersubband absorption in GaN/AlGaN step quantum wells," Appl. Phys. Lett. 97, 191101 (2010).

[11]   Bayram, C., Vashaei, Z., and Razeghi, M., "Reliability in room-temperature negative differential resistance characteristics of low-aluminum content AlGaN/GaN double-barrier resonant tunneling diodes," Appl. Phys. Lett. 97, 181109 (2010).

[12]   Gurnick, M. and DeTemple, T., "Synthetic nonlinear semiconductors," IEEE J. Quantum Electron., 19, 791-794 (1983).

[13]   Owschimikow, N., Gmachl, C., Belyanin, A., Kocharovsky, V., Sivco, D. L., Colombelli, R., Capasso, F., and Cho, A. Y., "Resonant Second-Order Nonlinear Optical Processes in Quantum Cascade Lasers," Phys. Rev. Lett., 90, 043902 (2003).

[14]   Belkin, M. A., Capasso, F., Belyanin, A., Sivco, D. L., Cho, A. Y., Oakley, D. C., Vineis, C. J., and Turner, G. W., "Terahertz quantum-cascade-laser source based on intracavity difference-frequency generation," Nat. Photonics, 1, 288-292 (2007).

[15]   Belkin, M. A., Capasso, F., Xie, F., Belyanin, A., Fischer, M., Wittmann, A., and Faist, J., "Room temperature terahertz quantum cascade laser source based on intracavity difference-frequency generation," Appl. Phys. Lett., 92, 201101 (2008).

[16]   Bai, Y., Slivken, S., Darvish, S. R., Haddadi, A., Gokden, B., and Razeghi, M., "High power broad area quantum cascade lasers," Appl. Phys. Lett., 95, 221104 (2009).

[17]   Geiser, M., Pflugl, C., Belyanin, A., Wang, Q. J., Yu, N. F., Edamura, T., Yamanishi, M., Kan, H., Fischer, M., Wittmann, A., Faist, J., and Capasso, F., "Gain competition in dual wavelength quantum cascade lasers," Opt. Express, 18, 9900-9908 (2010).